A Survey of Control Charts for Simple Linear Profile Processes with Autocorrelation

Jyun-You Chiang, Hon Keung Tony Ng, Tzong-Ru Tsai, Yuhlong Lio, and Ding-Geng Chen

Abstract In quality control, the quality of process or product can be characterized by a profile that defines as a functional relationship between a quality response variable and one or more explanatory variables. Many research works have been accomplished on statistical process control for simple linear profile with independent or autocorrelated observations. This chapter will serve as a review of some recent works on statistical quality control on autocorrelated simple linear profiles.

1 Introduction

In many statistical process control (SPC) applications, the quality of a product can be characterized by a functional relationship between a response variable and one or more independent variables. This functional relationship is often called profile. The profile that links a response variable to the explanation variables can be linear and nonlinear in nature. In statistical quality control, Jensen et al. [6] considered a general linear profile model with m profiles. We assume that there are n observations

J.-Y. Chiang (✉)
School of Statistics, Southwestern University of Finance and Economics, Chengdu, China
e-mail: jiangjy@swufe.edu.cn

H. K. T. Ng
Department of Statistical Science, Southern Methodist University, Dallas, TX, USA
e-mail: ngh@mail.smu.edu

T.-R. Tsai
Department of Statistics, Tamkang University, New Taipei City, Taiwan
e-mail: tzongru@gms.tku.edu.tw

Y. Lio
Department of Mathematical Sciences, University of South Dakota, Vermillion, SD, USA
e-mail: Yuhlong.Lio@usd.edu

D.-G. Chen
Department of Statistics, University of Pretoria, Pretoria, South Africa
e-mail: chend05@gmail.com

Y. Lio et al. (eds.), *Statistical Quality Technologies*, ICSA Book Series in Statistics,
https://doi.org/10.1007/978-3-030-20709-0_5

in each of the j-th profile, $j = 1, 2, \ldots, m$. The general linear profile model is defined as

$$\mathbf{y}_j = \boldsymbol{\gamma}_{0,j} + \mathbf{X}_j \boldsymbol{\gamma}_j + \mathbf{Z}_j \mathbf{b}_j + \boldsymbol{\epsilon}_j, \tag{1}$$

where $\mathbf{y}_j$ is a $n \times 1$ vector of responses, $\mathbf{X}_j$ is a $n \times p$ matrix of the regressor variables associated with the fixed effects, $\boldsymbol{\gamma}_j$ is a $p \times 1$ parameter vector of coefficients for the fixed effects, $\mathbf{Z}_j$ is a $n \times q$ matrix of predictors associated with random effects, $\mathbf{b}_j \sim MN(\mathbf{0}, \mathbf{D})$ is a $q \times 1$ vector of random effect coefficients, $MN(\mathbf{0}, \mathbf{D})$ denotes a multivariate normal distribution with zero mean vector $\mathbf{0}$ and positive definite variance-covariance matrix $\mathbf{D}$, $\boldsymbol{\epsilon}_j \sim MN(\mathbf{0}, \mathbf{R}_j)$ is a $n \times 1$ vector of errors, and $MN(\mathbf{0}, \mathbf{R}_j)$ is a multivariate normal distribution with zero mean vector $\mathbf{0}$ and positive definite variance-covariance matrix $\mathbf{R}_j$ for $j = 1, 2, \cdots, m$. If the errors are assumed to be independent, then $\mathbf{R}_j = \sigma^2 \mathbf{I}$ where $\mathbf{I}$ is the identity matrix. If the errors are correlated, $\mathbf{R}_j$ is often assumed as a simple form such as the autoregressive (AR) model in order to reduce the number of covariance parameters needed to be estimated. When Eq. (1) is reduced to the model that has only one fixed effect regressor variable and no random effect terms, the profile model is called a simple linear profile (SLP) model. The currently developed SPC on SLP models have been focused on the same levels of fixed effect regressor for all the profiles. Therefore, the SLP model can be defined as

$$y_{i,j} = \gamma_0 + x_i \gamma_1 + \epsilon_{i,j}, \tag{2}$$

where $y_{i,j}$ is the response in the j-th profile at the i-th level of predictor, x_i, γ_0 is the intercept, γ_1 is the model parameter for the predictor and $\epsilon_{i,j}$ are $N(0, \sigma^2)$ distributed for $i = 1, 2, \cdots, n$ and $j = 1, 2, \cdots, m$. SPC methods that involve monitoring a SLP process have drawn considerable attention over the past two decades because a SLP model is easy to handle and can be applied to many production processes. Process monitoring using control charts is a two-stage process, which has Phase I and Phase II. Phase I is to evaluate the stability of the process and estimate the in-control values of the process parameters, and Phase II is to monitor the future online data obtained after Phase I and detect shifts in the process parameters. In phase I, it is important to confirm the process stability under a given false alarm rate, i.e., a type-I error probability. In Phase II, the emphasis is on detecting process change as soon as possible. Both stages are usually measured by parameters, mean and standard deviation, of the run length distribution, where run length is the number of samples taken before an out-of-control signal is occurred. Therefore, the average run length (ARL_1) when the process out-of-control during the Phase II monitoring is often used to compare the performance of competing control chart methods under a given average run length ARL_0 for in-control Phase I. Numerous studies have been conducted on the use of profile monitoring methods, for example, Mestek et al. [11], Stover and Brill [17], Kang and Albin [7], Kim et al. [8], and Mahmoud et al. [10] studied some Phase I monitoring methods for SLP processes in order to set and evaluate the stability of a process and

to estimate process parameters. Kang and Albin [7], Kim et al. [8], Noorossana [13], Gupta et al. [5], Zou et al. [19], and Saghaei et al. [14] studied Phase II monitoring methods for SLP processes to detect shifts in the process parameters as soon as possible. Woodall et al. [18] reviewed the research papers related to SPC using profiles, provided examples of profile monitoring methods, identified some weaknesses in existing methods and proposed some new research directions. All the aforementioned studies have assumed that all the m profile models have the same n values of one fixed effect regressor variable, and the error terms in the models are independent and follow a normal distribution. When the error terms are not independent, Noorossana et al. [12] studied a SLP model with error terms that have a first-order autocorrelation structure between profiles and showed the impact on the ARL performance of the T^2 control chart proposed by Kang and Albin [7]. In Noorossana et al. [12], three methods based on exponentially weighted moving average/range (EWMA/R) and T^2 [7] and EWMA-3 [8] were provided to eliminate the effect of autocorrelation between profiles and the ARL. When the response variables are produced at set of points over time, the response of a profile are very often autocorrelated. In this case, Soleimani et al. [16] considered a SLP model with error terms that follow a first-order autoregressive model (AR(1)) within profile and suggested the use of Hotelling T^2 control charts and EWMA-type control charts, namely EWMA-3 charts, for monitoring SLP processes in the presence of within-profile autocorrelation. These charts are simple to detect process shifts in SLP processes. The simulation results in Soleimani et al. [16] showed that among many competitive methods, EWMA-type control charts are the most effective in detecting shifts in the intercept or slope of a SLP model. Three EWMA control charts are obtained for EWMA-3 charts by re-parameterizing the SLP model in terms of its intercept and slope. The intercept of the transformed SLP model being monitored is a linear combination of the intercept and slope in the original SLP model. The EWMA-3 charts of Soleimani et al. [16] are less sensitive if the original intercept and slope shift simultaneously in opposite directions. Chiang et al. [3] investigated an operational and effective Phase II monitoring method for a SLP model with error terms follow an AR(1) within-profile. In Chiang et al. [3], a new multivariate MEWMA control chart, namely MEWMA-SLP chart, was developed on the basis of the design of Lowry et al. [9] for quickly detecting process shifts associated with the original intercept or slope in the presence of within-profile autocorrelation.

In this chapter, we survey the work of SLP model with AR(1) autocorrelation for the error terms. The rest of this chapter is organized as follows. A SLP model with between-profile autocorrelation and EWMA-3 charts are reviewed in Sect. 2. In Sect. 3, a SLP model with within-profile autocorrelation is introduced along with the Hotelling T^2, EWMA-3 and MEWMA-SLP control charts for this SLP model. In Sect. 4, we present the construction of the two process capability indices studied by Chiang et al. [3]. In Sect. 5, Monte Carlo simulations are conducted to explore the performance of the MEWMA-SLP chart are discussed, and the applications of the proposed process capability indices are illustrated. Finally, conclusions are provided in Sect. 6.

2 SLP Model with Between-Profile Autocorrelated Error Terms

When the error terms in a SLP model satisfy the following autocorrelation structure

$$\epsilon_{i,j} = \rho\epsilon_{i,j-1} + a_{i,j},\ i = 1, 2, \cdots, n,\ \ j = 1, 2, \cdots, m, \tag{3}$$

where $a_{i,j}, i = 1, 2, \cdots, n, j = 1, 2, \cdots, m$ are independent and identically distributed normal random variables with mean 0 and variance σ^2 and the random error terms $\epsilon_{i,j}$ for $i = 1, 2, \cdots, n$ within the j-th profile are independent, then the SLP model is a SLP model with between-profile autocorrelation [12]. Based on the autocorrelation structure between errors defined in Eq. (3), Noorossana et al. [12] provided the following autocorrelation structure between two different profiles at the same level of x_i:

$$y_{i,j} - (\gamma_0 + x_i\gamma_1) = \rho(y_{i,j-1} - (\gamma_0 + x_i\gamma_1)) + a_{i,j}, \tag{4}$$

and the prediction equation, $\hat{y}_{i,j} = \rho y_{i,j-1} + (1 - \rho)(\gamma_0 + x_i\gamma_1)$. Although there exists an AR(1) structure between errors corresponding to each level of predictor in different profiles in Eq. (4), Noorossana et al. [12] showed that the residual $e_{i,j} = y_{i,j} - \hat{y}_{i,j}$ equates to $a_{i,j}$, for $i = 1, 2, \cdots, n$ and $j = 1, 2, \cdots, m$ and the residuals are independent random variables with the expected value $E(e_{i,j}) = 0$ and variance $var(e_{i,j}) = \sigma^2$. Hence, $e_{i,j}$ can be monitored using traditional control charts. Noorossana et al. [12] proposed three methods to monitor the residuals $e_{i,j}$ for $i = 1, 2, \cdots, n$ and $j = 1, 2, \cdots, m$. Let $\bar{e}_j = \sum_{i=1}^{n} e_{i,j}/n$ for the j-th profile. The three methods are reviewed as follows. When the model parameters are unknown, the corresponding maximum likelihood estimates can be used to replace the values of the model parameters to establish the control charts.

Method 1: EWMA Chart Combining with R-Chart for Monitoring the Error Variance

The first method is EWMA in combining with R-chart, which is the same as the control charts used by Kang and Albin [7]. The EWMA chart procedure is constructed as follows:

Step 1: Define the EWMA sequence using residuals, $e_{i,j}$ for $i = 1, 2, \cdots, n$ and $j = 1, 2, \cdots, m$, as $z_j = \theta\bar{e}_j + (1 - \theta)z_{j-1}$ with $0 < \theta < 1$ as a smoothing constant and $z_0 = 0$

Step 2: Define the lower control limit (LCL) and the upper control limit (UCL) for EWMA chart as $LCL_{EWMA} = -L\sigma\sqrt{\frac{\theta}{(2-\theta)n}}$ and $UCL_{EWMA} = L\sigma\sqrt{\frac{\theta}{(2-\theta)n}}$, where L is a positive constant selected to give a specified in-control ARL, ARL_0.

The R-chart to detect shifts in the process variance is constructed as follows:

Step 1: Define the R sequence as $R_j = max_i(e_{i,j}) - min_i(e_{i,j})$ for the j-th profile.

Step 2: Define the lower control limit (LCL) and the upper control limit (UCL) for the R chart as $LCL_R = \sigma(d_2 - Ld_3)$ and $UCL_R = \sigma(d_2 + Ld_3)$, where L is a positive constant chosen to give a specified in-control ARL_0 and the values of d_2 and d_3 are constants depending on the sample size n.

Method 2: Modified Hotelling T^2 Control Chart

The second method proposed by Noorossana et al. [12] is a modified Hotelling T^2 control chart studied by Kang and Albin [7]. The modified Hotelling T^2 control chart is described as follows:

Step 1: Define $T_j^2 = (\mathbf{e}_j - \mathbf{0})\Sigma^{-1}(\mathbf{e}_j - \mathbf{0})^T$ where $\mathbf{e}_j = (e_{1,j}, e_{2,j}, \cdots, e_{n,j})$, $\mathbf{0}$ is a $n \times 1$ zero vector, $\Sigma = \sigma^2\mathbf{I}$ and $\mathbf{I}$ is a $n \times n$ identity matrix.

Step 2: Define the upper control limit as $UCL_T = \chi^2_{n,\alpha}$, which is the $100(1-\alpha)$ percentile of the chi-square distribution with n degree of freedom.

Method 3: Modified EWMA-3

The third method proposed by Noorossana et al. [12] is a modified EWMA-3 studied by Kim et al. [8] which was designed to deal with the autocorrelation between profiles. Noorossana et al. [12] proposed the scaling of the x-variable such that the average x-value is zero and the transformed SLP model of Eq. (2) with autocorrelation in Eq. (3) is

$$y_{i,j} = b_0 + x_i^* b_1 + \epsilon_{i,j}, \epsilon_{i,j} = \rho\epsilon_{i,j-1} + a_{i,j}, \ i = 1, 2, \cdots, n, \ j = 1, 2, \cdots, m, \tag{5}$$

where $x_i^* = (x_i - \bar{x})$, $b_0 = \gamma_0 + \gamma_1\bar{x}$ and $\bar{x} = \sum_{i=1}^n x_i/n$. Noorossana et al. [12] showed that the AR(1) structure between observations can be transformed into the intercept and the slope estimators in the successive profiles. Let $\hat{b}_{0,j}$ be the least squared estimate for b_0 and $\hat{b}_{1,j}$ be the least squared estimate for b_1 using the sample from the j-th profile. Noorossana et al. [12] calculated the residual for the intercept as $e_0(j) = \hat{b}_{0,j} - \rho\hat{b}_{0,j-1} - (1-\rho)b_0$, the residual for the slope as $e_1(j) = \hat{b}_{1,j} - \rho\hat{b}_{1,j-1} - (1-\rho)b_1$, and the residual as $e_{i,j} = y_{i,j} - \hat{y}_{i,j} = y_{i,j} - \rho y_{i,j-1} - (1-\rho)(b_0 + b_1 x_i^*)$, then the mean squared error (MSE) is defined as $MSE_j = \sum_{i=1}^n e_{i,j}^2/n$ for the j-th profile. The process of EWMA-3 that contains three control charts is described as follows:

Step 1: EWMA-3 for monitoring the intercept b_0 is established as follows:

1.1 Define $EWMA_0(j) = \theta e_0(j) + (1-\theta)EWMA_0(j-1)$, where $0 < \theta \leq 1$ is a smoothing constant and $EWMA_0(0) = 0$.

1.2 Define the lower control limit (LCL) and upper control limit (UCL) respectively as $LCL_1 = -L_0\sigma\sqrt{\theta/[(2-\theta)n]}$ and $UCL_1 = L_0\sigma\sqrt{\theta/[(2-\theta)n]}$, where $L_0 > 0$ is chosen to give a specified in-control ARL_0.

Step 2: EWMA-3 for monitoring the slop b_1 is established as follows:

2.1 Define $EWMA_1(j) = \theta e_1(j) + (1-\theta)EWMA_1(j-1)$, where $0 < \theta \leq 1$ is a smoothing constant and $EWMA_1(0) = 0$.

2.2 Define the lower control limit (LCL) and upper control limit (UCL) respectively as $LCL_2 = -L_1\sigma\sqrt{\theta/[(2-\theta)\sum_{i=1}^{n} x_i^{*2}]}$ and $UCL_2 = L_1\sigma\sqrt{\theta/[(2-\theta)\sum_{i=1}^{n} x_i^{*2}]}$, where $L_1 > 0$ is chosen to give a specified in-control ARL_0.

Step 3: EWMA-3 for monitoring the error variance is established as follows:

3.1 Define $EWMA_E(j) = \max\{\theta(MSE_j - 1) + (1-\theta)EWMA_E(j-1), 0\}$ with $0 < \theta \leq 1$ as a smoothing constant and $EWMA_E(0) = 0$

3.2 Define the upper control limit as $UCL_3 = L_E\sqrt{\theta Var(MSE_j)/(2-\theta)}$ where $Var(MSE_j) = Var(\sum_{i=1}^{n} e_{i,j}^2/n) = 2\sigma^4/n$ and $L_E > 0$ is chosen to give a specified in-control ARL_0.

3 SLP Model with Within-Profile Autocorrelated Error Terms

When the error terms in a SLP model satisfy the following autocorrelation structure

$$\epsilon_{i,j} = \rho\epsilon_{i-1,j} + a_{i,j},\ i = 1, 2, \cdots, n,\ j = 1, 2, \cdots, m, \tag{6}$$

where $a_{i,j}, i = 1, 2, \cdots, n, j = 1, 2, \cdots, m$ are independent and identically distributed normal random variables with mean 0 and variance σ^2 and the random error terms $\epsilon_{i,j}$ for $j = 1, 2, \cdots, m$ between any two different profiles are independent, then the SLP model is a SLP model with within-profile autocorrelation. Let $y'_{i,j} = y_{i,j} - \rho y_{i-1,j}$, then the model based on Eqs. (2) and (6) can be expressed as

$$y'_{i,j} = \gamma'_0 + \gamma'_1 x'_i + a_{i,j},\ i = 2, 3, \cdots, n,\ j = 1, 2, \cdots, m, \tag{7}$$

where $\gamma'_0 = \gamma_0(1-\rho)$, $\gamma'_1 = \gamma_1$, and $x'_i = x_i - \rho x_{i-1}$. If the model parameters are unknown, they are replaced with their corresponding maximum likelihood estimates. In the Phase II monitoring, the model parameters γ_0, γ_1, σ^2, and ρ are treated as known constants. We define the residuals for the j-th profile as $e_{i,j} = y'_{i,j} - \gamma'_0 - \gamma'_1 x'_i$, $i = 1, 2, \cdots, n$. Following the approach proposed by Kang and Albin [7] for monitoring independent SLP processes, Soleimani et al. [16] proposed the four control charts, T^2 method, T^2 based on the residuals, EWMA/R and EWMA-3, based on the residuals from the transformed model in Eq. (7) to

monitor SLP processes with within-profile autocorrelation. The first two Hotelling T^2 charts are stated as follows:

Hotelling T^2 Method for the Transformed Model

Step 1: Let $\hat{\gamma}'_{0,j}$ and $\hat{\gamma}'_{1,j}$ be the respective estimators of γ'_0 and γ'_1 based on the jth profile sample.

Step 2: Define $T_j^2 = [\hat{\gamma}'_{0,j}, \hat{\gamma}'_{1,j}] - [\gamma'_{0,j}, \gamma'_{1,j}]^T S^{-1} [\hat{\gamma}'_{0,j}, \hat{\gamma}'_{1,j}] - [\gamma'_{0,j}, \gamma'_{1,j}]$, where

$$S = \begin{bmatrix} \sigma^2(1/(n-1) + \bar{x}'^2/s_{x'x'}) & -\sigma_2 \bar{x}'/s_{x'x'} \\ -\sigma_2 \bar{x}'/s_{x'x'} & \sigma_2/s_{x'x'} \end{bmatrix}.$$

Step 3: Under in-control process, T^2 has a central chi-square distribution of two degree freedom. Therefore, the upper control limit (UCL) for the chart is $UCL = \chi^2_{2,\alpha}$, where $\chi^2_{2,\alpha}$ is the $100(1-\alpha)$-th percentile of the chi-square distribution with two degree of freedom.

Hotelling T^2 Method Based on the Residuals from the Transformed Model

Step 1: Define $T_j^2 = (\mathbf{e}_j - \mathbf{0})\Sigma^{-1}(\mathbf{e}_j - \mathbf{0})^T$ where $\mathbf{e}_j = (e_{1,j}, e_{2,j}, \cdots, e_{n,j})$, $\mathbf{0}$ is a $n \times 1$ vector of zeros, $\Sigma = \sigma^2\mathbf{I}$ and $\mathbf{I}$ is a $n \times n$ identity matrix.

Step 2: Define upper control limit as $UCL = \chi^2_{n-1,\alpha}$, which is the $100(1-\alpha)$-th percentile of the chi-square distribution with $n-1$ degree of freedom.

The EWMA-3 charts for the intercept, slope, and the variance of error terms [16] can be respectively constructed using the following three charting processes:

Control Chart 1: EWMA-3 Chart for Monitoring the Intercept

The first EWMA-3 chart, namely the EWMA-3I chart, is constructed using the following steps:

Step 1: Let $B_0 = \gamma'_0 + \gamma'_1\bar{x}'$, $B_1 = \gamma'_1$, $x''_i = (x'_i - \bar{x}')$, and express the model in Eq. (7) as

$$y'_{i,j} = B_0 + B_1 x''_i + a_{i,j},\ i = 1, 2, \cdots, n,\ j = 1, 2, \cdots, m. \tag{8}$$

Step 2: Derive the EWMA sequence of the B_0 estimates from the equation

$$\omega_I(j) = \theta b_{0,j} + (1-\theta)\omega_I(j-1),\ j = 1, 2, \cdots, m,$$

where $b_{0,j}$ is the least squares estimate obtained based on the observations in the j-th subgroup. Furthermore, $\omega_I(0) = B_0$, and θ $(0 < \theta \leq 1)$ is a smoothing constant. The control limits can be represented as

$$LCL_I = B_0 - L_I\sigma\sqrt{\frac{\theta}{(2-\theta)(n-1)}}$$

and

$$UCL_I = B_0 + L_I\sigma\sqrt{\frac{\theta}{(2-\theta)(n-1)}},$$

where $L_I(>0)$ is a control chart parameter.

Control Chart 2: EWMA-3 Chart for Monitoring the Slope
The second EWMA-3 chart, namely the EWMA-3S chart, is constructed using the following steps:

Step 1: On the basis of the transformations of B_0, B_1, and x_i'' in Eq. (8), the EWMA sequence of the B_1 estimates can be derived through

$$\omega_S(j) = \theta b_{1,j} + (1-\theta)\omega_S(j-1),\ \ j = 1, 2, \cdots, m,$$

where $\omega_S(0) = B_1$, and $b_{1,j}$ is the least squares estimate obtained based on the observations in the j-th subgroup.

Step 2: The control limits can be obtained as

$$LCL_S = B_1 - L_S\sigma\sqrt{\frac{\theta}{(2-\theta)S_{xx}}}$$

and

$$UCL_S = B_1 + L_S\sigma\sqrt{\frac{\theta}{(2-\theta)S_{xx}}},$$

where $S_{xx} = \sum_{i=2}^{n} x_i''^2$ and $L_S(>0)$ is a control chart parameter.

Control Chart 3: EWMA-3 Chart for Monitoring the Error Variance
The third chart, namely the EWMA-3e chart, is constructed using the following steps:

Step 1: Evaluate the MSE for each profile as

$$MSE_j = \frac{\sum_{i=2}^{n} e_{i,j}^2}{n-1},\ \ j = 1, 2, \cdots, m.$$

Step 2: The EWMA sequence of MSE_j can be derived through

$$\omega_E(j) = \max\{\theta(MSE_j - 1) + (1-\theta)\omega_E(j-1), 0\},\ \ j = 1, 2, \cdots, m,$$

where $\omega_E(0) = 0$. The upper control limit can be obtained as

$$UCL = L_E\sqrt{\frac{\theta Var(MSE_j)}{2-\theta}},$$

where

$$Var(MSE_j) = \frac{2\sigma^4}{n-1}$$

and $L_E(>0)$ is a control chart parameter.

The control chart parameters L_I, L_S, and L_E in the three EWMA-3 charts can be determined numerically such that a specified in-control average run length ARL_0 is reached.

3.1 MEWMA-SLP Chart

For the SLP model defined in Eqs. (2) and (6), the variance-covariance matrix of the error terms can be represented as $\sigma^2\Psi$, where

$$\Psi = \frac{1}{1-\rho^2}[\psi_{i,j}], \tag{9}$$

$\psi_{k,l} = 1$ for $k = l$, and $\psi_{k,l} = \rho^{(l-k)}$ for $k < l$. For each subgroup of size n, the SLP model in Eqs. (2) and (6) can be represented by $\mathbf{Y} = \mathbf{X}\boldsymbol{\gamma} + \boldsymbol{\epsilon}$, where $\mathbf{Y}^T = (y_1, y_2, \cdots, y_n)$, $\mathbf{X} = (\mathbf{1}, \mathbf{x})$, $\mathbf{1}$ is a $n \times 1$ vector with entries 1, $\mathbf{x}^T = (x_1, x_2, \cdots, x_n)$, $\boldsymbol{\gamma}^T = (\gamma_0, \gamma_1)$, and $\boldsymbol{\epsilon}^T = (\epsilon_1, \epsilon_2, \cdots, \epsilon_n)$. Because of Ψ is a positive definite matrix, the linear model can be expressed as $\mathbf{Y}_* = \mathbf{X}_*\boldsymbol{\gamma} + \boldsymbol{\epsilon}_*$, where $\mathbf{Y}_* = \Psi^{-1/2}\mathbf{Y}$, $\mathbf{X}_* = \Psi^{-1/2}\mathbf{X}$ and $\boldsymbol{\epsilon}_* = \Psi^{-1/2}\boldsymbol{\epsilon}$. Chiang et al. [3] mentioned that $E(\boldsymbol{\epsilon}_*) = \mathbf{0}$ and $Cov(\boldsymbol{\epsilon}_*) = \sigma^2 I$, where $\mathbf{0}$ is an order n column vector with entries 0 and I is an order n identity matrix. The generalized least squares (GLS) estimator of the model parameters γ_0 and γ_1, $\boldsymbol{\gamma}_G^T = (\hat{\gamma}_{G0}, \hat{\gamma}_{G1})$, of $\boldsymbol{\gamma}^T$, can be obtained as

$$\hat{\boldsymbol{\gamma}}_G = (\mathbf{X}_*^T\mathbf{X}_*)^{-1}\mathbf{X}_*^T\mathbf{Y} = (\mathbf{X}^T\Psi^{-1}\mathbf{X})^{-1}\mathbf{X}^T\Psi^{-1}\mathbf{Y}. \tag{10}$$

Chiang et al. [3] constructed the MEWMA-SLP chart based on the design of Lowry et al. [9] using the GLS estimates obtained from the Phase I samples of SLP process. The control chart procedure can be described as follows:

MEWMA-SLP Chart

Step 1: Obtain the GLS estimates $\hat{\boldsymbol{\gamma}}_{G,j}$ for $j = 1, 2, \cdots, m$ using Eq. (10) and the Phase I samples of SLP process.

Step 2: Compute $\bar{\hat{\boldsymbol{\gamma}}}_G = \sum_{j=1}^{m} \hat{\boldsymbol{\gamma}}_{G,j}/m = (\bar{\hat{\gamma}}_{G0}, \bar{\hat{\gamma}}_{G1})^T$. Let S_0 and S_1 denote the sample standard deviation of $\hat{\gamma}_{G0,j}$ and $\hat{\gamma}_{G1,j}$, $j = 1, 2, \cdots, m$, respectively, and let $\mathbf{U}_j$ be the rescaled vector of $\hat{\boldsymbol{\gamma}}_{G,j}$ for $j = 1, 2, \cdots, m$, where the rescaling involves the use of $\bar{\hat{\boldsymbol{\gamma}}}_G$, S_0, and S_1. The sample variance-covariance matrix of $\mathbf{U}_j$'s, denoted by $\mathbf{S}_\mathbf{U}$, can be obtained as

$$\mathbf{S}_\mathbf{U} = \frac{1}{m-1} \sum_{j=1}^{m} (\mathbf{U}_j - \bar{\mathbf{U}})(\mathbf{U}_j - \bar{\mathbf{U}})^T,$$

where $\bar{\mathbf{U}}$ is the sample mean of $\mathbf{U}_j$, $j = 1, 2, \cdots, m$.

Step 3: Derive the chart parameters κ ($0 < \kappa \leq 1$), and $UCL(= H)$ from the values suggested by Lowry et al. [9] for an in-control $ARL_0 = 200$. Useful parameter combinations are outlined as (κ, H) = (0.2, 9.65), (0.4, 10.29), (0.6, 10.53) and (0.8, 10.58). Other chart parameters can be obtained from the study of Lowry et al. [9] or through Monte Carlo simulations.

Step 4: Compute the EWMA series of $\mathbf{U}_j$ from

$$\mathbf{Z}_j = \kappa \mathbf{U}_j + (1-\kappa)\mathbf{Z}_{j-1}, \ \ j = 1, 2, \cdots, m,$$

and the test statistics from

$$T_i^2 = \mathbf{Z}_i^T \mathbf{S}_{\mathbf{Z}_i}^{-1} \mathbf{Z}_i, \ \ j = 1, 2, \cdots, m,$$

where

$$\mathbf{S}_{\mathbf{Z}_j} = \frac{\kappa}{2-\kappa}[1-(1-\kappa)^{2j}]\mathbf{S}_\mathbf{U} \rightarrow \frac{\kappa}{2-\kappa}\mathbf{S}_\mathbf{U} \text{ as } j \text{ goesto } \infty.$$

4 Process Capability Indices

The process capability indices C_P and C_{PK} are widely used to evaluate the capability of a univariate process. These indices are defined as $C_P = (U-L)/6\sigma$ and $C_{PK} = \min\{U-\mu, \mu-L\}/3\sigma$, where L and U are the lower and upper specification limits of the univariate process characteristic quality and μ and σ are the mean and standard deviation of the process, respectively. For two-dimensional processes, C_P and C_{PK} are denoted by BC_P and BC_{PK}, respectively. The evaluations of BC_P and BC_{PK} for SLP processes are described as follows.

Let $\hat{\boldsymbol{\gamma}}_{G,j}$, $j = 1, 2, \cdots, m$ be the GLS estimators of the of the model parameters $\boldsymbol{\gamma} = (\gamma_0, \gamma_1)$ obtained by using the j-th in-control subgroups of the SLP process and the specification limits of γ_0 and γ_1 be labeled as (L_1', U_1') and (L_2', U_2'), respectively. Chiang et al. [3] improved the method proposed by Castagliola and Garcia Castellanos [2] through the following two steps:

Step 1: Let $\mathbf{U}_j$ be the bivariate vectors defined in the Step 2 of MEWMA-SLP, and let $L_1 = (L_1' - \bar{\hat{\gamma}}_{G0})/S_1$, $U_1 = (U_1' - \bar{\hat{\gamma}}_{G0})/S_1$, $L_2 = (L_2' - \bar{\hat{\gamma}}_{G1})/S_2$, and $U_2 = (U_2' - \bar{\hat{\gamma}}_{G1})/S_2$. Derive the bivariate process capability indices from $\mathbf{U}_j$, $j = 1, 2, \cdots, m$, L_1, U_1, L_2, and U_2.

Step 2: Use an orthogonal decomposition method to obtain the variance-covariance matrix of $\mathbf{U}_j$, $j = 1, 2, \cdots, m$. The variance-covariance matrix is given by

$$\mathbf{S}_{\mathbf{U}} = \mathbf{R}\Lambda\mathbf{R}^T, \tag{11}$$

where Λ is a diagonal matrix of rank two with eigenvalues $\lambda_1 < \lambda_2$ of $\mathbf{S}_{\mathbf{U}}$ as the diagonal elements. Furthermore, $\mathbf{R} = [\mathbf{r}_1^T, \mathbf{r}_2^T]$, where $\mathbf{r}_1^T = (r_{1,1}, r_{2,1})$ and $\mathbf{r}_2^T = (r_{1,2}, r_{2,2})$ are the eigenvectors corresponding to λ_1 and λ_2, respectively.

Let D_1 and D_2 be two lines passing through the point $G(\hat{\gamma}_{G0}, \hat{\gamma}_{G1})$ in the directions of the eigenvectors $\mathbf{r}_1$ and $\mathbf{r}_2$, respectively. The lines D_1 and D_2 split the $(\hat{\gamma}_{G0}, \hat{\gamma}_{G1})$-plane into four disjoint areas, which are denoted by A_1, A_2, A_3, and A_4 (see, Fig. 1). Because of $\hat{\boldsymbol{\gamma}}_G$ follows a bivariate normal (BVN) distribution which is symmetric about its mean $\boldsymbol{\beta}$, we can show that $P(\hat{\boldsymbol{\gamma}}_G \in A_i) = 1/4$, $i = 1, 2, 3$, and 4. Let

$$A = \{(\hat{\gamma}_{G0}, \hat{\gamma}_{G1}) | L_1 \le \hat{\gamma}_{G0} \le U_1,\ L_2 \le \hat{\gamma}_{G1} \le U_2\} = Q_1 \cup Q_2 \cup Q_3 \cup Q_4,$$

where $Q_i = A \cap A_i$ for $i = 1, 2, 3$, and 4. Let $q = P(\hat{\boldsymbol{\gamma}}_G \in A)$ and $p = 1 - q$, where p is the proportion of non-conformity. Furthermore, let $q_i = P(\hat{\boldsymbol{\gamma}}_G \in Q_i)$ and $p_i = P(\hat{\boldsymbol{\gamma}}_G \in A_i) - q_i = 1/4 - q_i$ for $i = 1, 2, 3$, and 4. Hence, $q =$

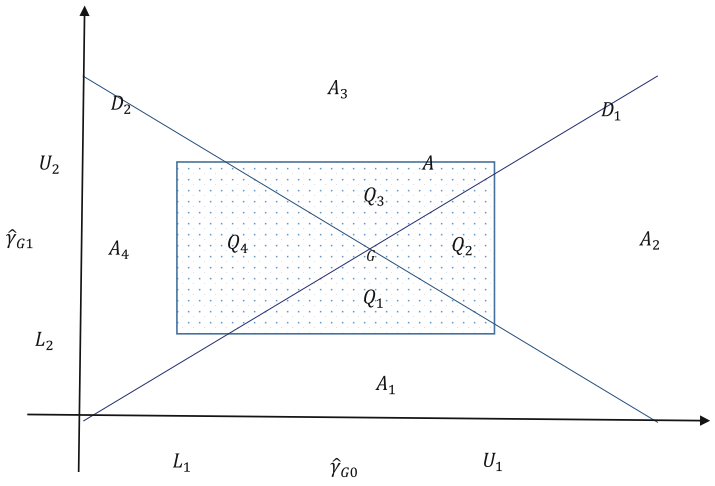

Fig. 1 The lines D_1 and D_2, and polygons Q_i for $i = 1, 2, 3, 4$

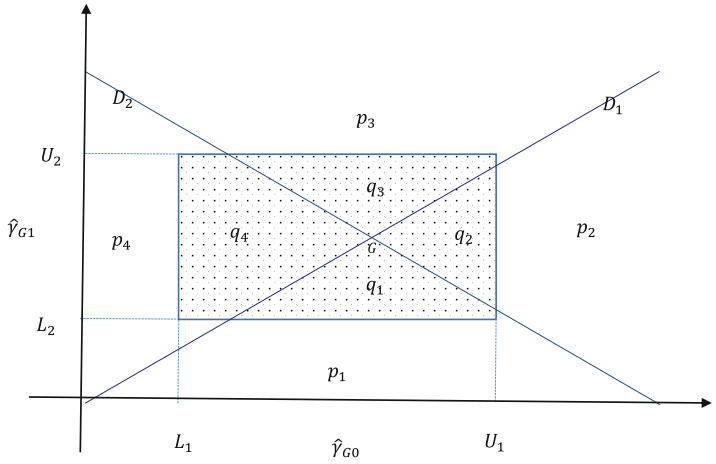

Fig. 2 The probabilities of p_i and q_i for $i = 1, 2, 3, 4$

$q_1 + q_2 + q_3 + q_4$ and $p = p_1 + p_2 + p_3 + p_4$ (Fig. 2). When the means of $\hat{\gamma}_{G0}$ and $\hat{\gamma}_{G1}$ are considered as the midpoints of their respective specification limits, then $p_1 = p_2 = p_3 = p_4 = p/4$ and $q_1 = q_2 = q_3 = q_4 = q/4$. According to the method presented in [2], the process capability indices for the GLS estimator $\hat{\boldsymbol{\gamma}}_G$ can be defined as

$$BC_P = -\frac{1}{3}\Phi^{-1}(p/2)$$

and

$$BC_{PK} = \min\{-\Phi^{-1}(2p_1), -\Phi^{-1}(2p_2), -\Phi^{-1}(2p_3), -\Phi^{-1}(2p_4)\},$$

where $\Phi(\cdot)$ is the cumulative distribution function of the standard normal distribution. Chiang et al. [3] suggested that the probabilities p_i and q_i, $i = 1, 2, 3$, and 4, can be obtained using the R packages `mvtnorm:pmvnorm` [4] and `pracma:triquad` [1] and they proposed the following two algorithms to obtain BC_P and BC_{PK}.

Algorithm A: Evaluation of BC_{PK}

Step 1: Obtain $\mathbf{U}_j$, L_1, U_1, L_2, and U_2, then evaluate the sample variance-covariance matrix $\mathbf{S}_\mathbf{U}$ from $\mathbf{U}_j$, $j = 1, 2, \cdots, m$.

Step 2: Find the diagonal matrix Λ of eigenvalues and the matrix of eigenvectors $\mathbf{R}$ from the orthogonal decomposition $\mathbf{S}_\mathbf{U} = \mathbf{R}\Lambda\mathbf{R}^T$.

Step 3: Let $\mathbf{c}_1, \mathbf{c}_2, \cdots, \mathbf{c}_\ell$ be the vertices of the polygon Q_i, then obtain the transformed vertices of Q_i through $\mathbf{c}_l' = \mathbf{R}\Lambda^{-1/2}\mathbf{R}^T\mathbf{c}_l$ for $l = 1, 2, \cdots, \ell$.

Step 4: Determine the probabilities $\hat{q}_i$ and $p_i (= 1/4 - q_i)$ for $i = 1, 2, 3$, and 4.

Step 5: Estimate BC_{PK} as

$$\hat{BC}_{PK} = \frac{1}{3}\min\{-\Phi^{-1}(2\hat{p}_1), -\Phi^{-1}(2\hat{p}_2), -\Phi^{-1}(2\hat{p}_3), -\Phi^{-1}(2\hat{p}_4)\}.$$

Algorithm B: Evaluation of BC_P

Step 1: Let $\hat{\boldsymbol{\gamma}}_{G,j}$ for $j = 1, 2, \cdots, m$ follow a $BVN(\boldsymbol{\mu}_B, \mathbf{S}_{\boldsymbol{\gamma}})$ distribution with mean $\boldsymbol{\mu}_B = ((L_1' + U_1')/2, (L_2' + U_2')/2)$ and variance-covariance matrix

$$\mathbf{S}_{\boldsymbol{\gamma}} = \frac{1}{m-1}\sum_{j=1}^{m}(\hat{\boldsymbol{\gamma}}_{G,j} - \boldsymbol{\mu}_B)(\hat{\boldsymbol{\gamma}}_{G,j} - \boldsymbol{\mu}_B)^T,$$

and denote the probability density function of $BVN(\boldsymbol{\mu}_B, \mathbf{S}_{\boldsymbol{\gamma}})$ distribution as $f(\hat{\gamma}_0, \hat{\gamma}_1)$.

Step 2: Evaluate the probability

$$\hat{q} = \int_{L_1'}^{U_1'}\int_{L_2'}^{U_2'} f(t_1, t_2)dt_1dt_2,$$

and $\hat{p} = 1 - \hat{q}$.

Step 3: Estimate BC_P as

$$\hat{BC}_P = -\frac{1}{3}\Phi^{-1}(\hat{p}/2).$$

5 Monte Carlo Simulation Study and Numerical Example

5.1 Monte Carlo Simulation Study

To evaluate the performance of the MEWMA-SLP chart, Chiang et al. [3] used the model settings as described in [15]. Let $\gamma_0 = 3$ and $\gamma_1 = 2$ for the models in Eqs. (2) and (6). The points set for Eq. (2) are $x_i = 2, 4, 6$, and 8. Because Soleimani et al. [16] revealed that the EWMA-3 charts outperform other competitive methods, we only compare the performance of the EWMA-3 charts with the MEWMA-SLP chart.

The EWMA-3 charts use EWMA-3I, EWMA-3S and EWMA-3e charts to simultaneously monitor the intercept, slope, and error variance of a SLP model. The overall false alarm rate of EWMA-3 charts can be determined as

$$\alpha_{EWMA} = 1 - (1 - \alpha_1')(1 - \alpha_2')(1 - \alpha_3'),$$

where α_1', α_2' and α_3' are the false alarm rates for EWMA-3I, EWMA-3S and EWMA-3e, respectively. Chiang et al. [3] used the MEWMA-SLP chart and the EWMA-3e chart simultaneously to monitor the intercept, slope, and error variance of a SLP model. The overall false alarm rate of can be obtained as

$$\alpha_{MEWMA} = 1 - (1 - \alpha_1)(1 - \alpha_2),$$

where α_1 and α_2 are the false alarm rates of the MEWMA-SLP and EWMA-3e charts, respectively. Because the EWMA-3e chart is used to monitor the error variance for both approaches, the performance of the EWMA-3e chart is omitted in the comparison. Specifically, the error variance was assumed to be in a statistical control state in the simulation study. Hence, Chiang et al. [3] only compared the performance of monitoring SLP process based on the EWMA-3I and EWMA-3S charts with the performance of monitoring SLP process based on the MEWMA-SLP chart.

In the simulation study, the correlation coefficient between the adjacent error terms, ρ, is set to be 0.1, 0.7 or 0.9, and the overall ARL_0 is set to be 200 (i.e., the overall false alarm rate $\alpha = 0.005$). Without loss of generality, let $\alpha_1' = \alpha_2' = 1 - \sqrt{1-\alpha} \cong 0.0025$ for the EWMA-3I and EWMA-3S charts, and let $\alpha_1 = \alpha_2 = 0.005$ for the MEWMA-SLP chart. The chart parameters of the MEWMA-SLP chart are set as $\kappa = 0.2$ and $H = 9.65$.

In Phase I monitoring for the model parameter, estimation of the parameters is involved in using the EWMA-3I and EWMA-3S charts and 10,000 in-control SLP processes were prepared. A simulation with 10,000 iterations was conducted to obtain the chart parameters, which are $L_I = 2.889$ and $L_S = 2.895$, for using the EWMA-3I and EWMA-3S simultaneously to achieve an approximated overall ARL_0 of 200. The EWMA-3 charts and the MEWMA-SLP chart were constructed in Phase I. The out-of-control average run length, denoted by ARL_1, was evaluated for different parameter shifts in the Phase II monitoring.

Two scenarios were considered for the parameter shift. Scenario I (SI) was set to be same as the simulation setting of Soleimani et al. [16]. In SI, the shift in either the intercept or the slope of a SLP model was considered, and the other parameter kept unchanged. In scenario II (SII), the shifts in both the intercept and the slope of a SLP model were considered simultaneously. Assume that the intercept shifts from γ_0 to $\gamma_0' = \gamma_0 + \lambda\sigma$ and the slope shifts from γ_1 to $\gamma_1' = \gamma_1 + \beta\sigma$ when an assignable cause is introduced. Here, λ and β are two constants. The parameter combinations for SI are (1) $\lambda = 0.2, 0.4, 0.6, 0.8, 1, 1.2, 1.4, 1.6, 1.8$ and 2, and $\beta = 0$; and (2) $\beta = 0.025, 0.05, 0.075, 0.1, 0.125, 0.15, 0.175, 0.2, 0.225$ and 0.25, and $\lambda = 0$.

In many practical applications, an intercept shift often accompanies with a slope shift for a SLP process. Figure 3 presents an example, in which the nominal regression line is characterized by the conditional expected value of y, given x, as follows:

$$\mu(y|x) = \gamma_0 + \gamma_1 x. \tag{12}$$

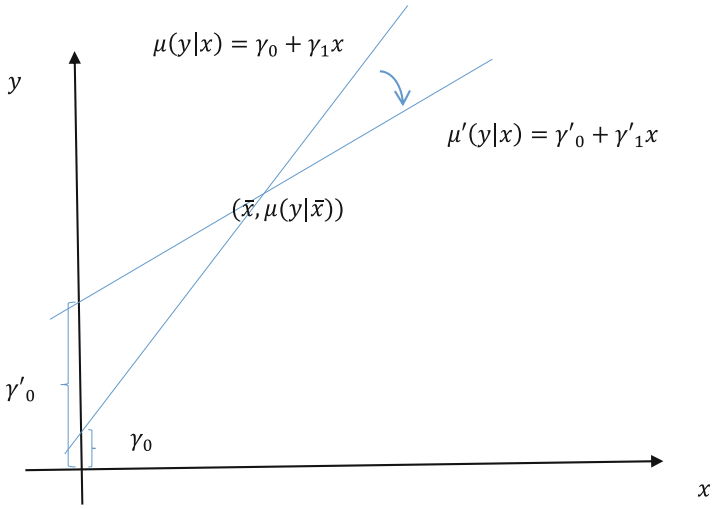

Fig. 3 An example of an intercept shift accompanies a slope shift for a SLP

When the profile parameters shift because of an assignable cause, the nominal regression line shifts to

$$\mu'(y|x) = \gamma_0' + \gamma_1' x. \tag{13}$$

In Fig. 3, both $\mu(y|x)$ and $\mu'(y|x)$ pass through the point $(P_x, P_y), = (\bar{x}, \mu(y|\bar{x}))$. Using $(P_x, P_y) = (\bar{x}, \mu(y|\bar{x}))$ in Eqs. (12) and (13), we can obtain

$$P_y = \gamma_0 + \gamma_1 \bar{x}$$

and

$$\gamma_0' = (\gamma_0 + \gamma_1 \bar{x}) - \gamma_1' \bar{x}. \tag{14}$$

Because $\gamma_0 = 3$, $\gamma_1 = 2$, and $x_i = 2, 4, 6, 8$, Eq. (14) reduces to

$$\gamma_0' = 13 - 5\gamma_1'. \tag{15}$$

To present the process shifts on the σ scale, Chiang et al. [3] obtained $\gamma_0' = \gamma_0 + \lambda\sigma = 3 + \lambda$ and $\gamma_1' = \gamma_1 + \beta\sigma = 2 + \beta$. Subsequently substituting $\gamma_0' = 3 + \lambda$ and $\gamma_1' = 2 + \beta$ into Eq. (15) yields the relationship between λ and β as $\lambda = -5\beta$. In the study conducted by Chiang et al. [3], $\beta = -0.50, -0.46, -0.44, -0.42, -0.40, -0.38, -0.36, -0.34, -0.32, -0.30, -0.28, -0.26, -0.24, -0.22, -0.20, -0.18, -0.16, -0.14, -0.12, -0.10, -0.08, -0.06, -0.04$, and -0.02 in the simulation for determining the speed of control charts

for detecting process shifts. The values of λ can be obtained using the relation $\lambda = -5\beta$. The out-of-control ARL, denoted by ARL_1, was evaluated through a simulation with 10,000 realizations. A single alarm of the EWMA-3I or the EWMA-3S indicates that the process is out of control for EWMA-3. The value of ARL_1 obtained from this charting procedure is labeled as ARL_1-$E3$, and the value of ARL_1 determined from MEWMA-SLP is labeled as ARL_1-ME.

The Monte Carlo simulation study presented in [3] clearly showed that the MEWMA-SLP chart outperforms EWMA-3I and EWMA-3S simultaneous charting. The MEWMA-SLP chart is faster than the combined EWMA-3I and EWMA-3S charts in detecting the process shift for the two scenarios considered. In particular, the simulation results show that the MEWMA-SLP chart improves the performance of the combined EWMA-3I and EWMA-3S charts considerably when ρ is close to 1. When $\rho = 0.9$, the sensitivity of the combined EWMA-3I and EWMA-3S charts in detecting a process shift engendered by an intercept shift was low. More detail information, interested readers are suggested to read Chiang et al. [3].

5.2 Numerical Example

When a SLP process is identified as in-control, the process capability should be evaluated. To illustrate the application of the two new process capability indices, Chiang et al. [3] generated data sets of size $m = 200$ with ρ =0.1, 0.7, and 0.9 based on the model in Eqs. (2) and (6) with $\gamma_0 = 3$ and $\gamma_1 = 2$. Let the lower and upper specification limits of the response variable y be LSL_y and USL_y, respectively. If the mean of y, given $x = \bar{x}$, is the midpoint of the specification limits, then LSL_y and USL_y can be expressed as

$$LSL_y = E(y|x = \bar{x}) - k\sigma = \gamma_0 + \gamma_1\bar{x} - k_1\sigma \tag{16}$$

and

$$USL_y = E(y|x = \bar{x}) + k\sigma = \gamma_0 + \gamma_1\bar{x} + k_2\sigma, \tag{17}$$

respectively. Using Eqs. (16) and (17), Chiang et al. [3] obtained

$$\gamma_0 = \frac{LSL_y + USL_y - (k_2 - k_1)\sigma}{2} - \gamma_1\bar{x},$$

$$\gamma_1 = \frac{\frac{LSL_y + USL_y - (k_2 - k_1)\sigma}{2} - \gamma_0}{\bar{x}},$$

$LSL_y - (k_2 - k_1)\sigma/2 - \gamma_1\bar{x} \le \gamma_0 \le USL_y - (k_2 - k_1)\sigma/2 - \gamma_1\bar{x}$ and $(LSL_y - (k_2 - k_1)\sigma/2 - \gamma_0)/\bar{x} \le \gamma_1 \le (USL_y - (k_2 - k_1)\sigma/2 - \gamma_0)/\bar{x}$. On the basis of the specification limits of the response variable, the specifications limits of $\hat{\gamma}_{G0}$ and $\hat{\gamma}_{G1}$ can be expressed as

$$LSL_{G0} = LSL_y - \gamma_1\bar{x},$$

$$USL_{G0} = USL_y - \gamma_1\bar{x},$$

and

$$LSL_{G1} = \frac{LSL_y - \gamma_0}{\bar{x}},$$

$$USL_{G1} = \frac{USL_y - \gamma_0}{\bar{x}}.$$

When the parameters γ_0 and γ_1 are unknown, the parameters γ_0 and γ_1 can be replaced with the sample means of $\hat{\gamma}_{G0,j}$ and $\hat{\gamma}_{G1,j}$, respectively.

In the numerical examples, let $k_1 = 4$, $k_2 = 3.5$, $LSL_y = 9$, $USL_y = 16.5$, $LSL_{G0} = LSL_y - \gamma_1\bar{x} = -0.75$, $USL_{G0} = USL_y - \gamma_1\bar{x} = 6.75$, $LSL_{G1} = LSL_y - \gamma_0/\bar{x} = 1.25$, and $USL_{G1} = USL_y - \gamma_0/\bar{x} = 2.75$. Chiang et al. [3] studied the relationship between ρ and the process capability indices BC_p and BC_{pk}. The study showed that BC_p and BC_{pk} were influenced by the with-profile correlation and they are overestimated if the with-profile correlation was ignored. Furthermore, the maximal values of BC_p and BC_{pk} were attained for $\rho = 0$. The value of BC_{pk} decreases as ρ increases and the values of BC_p and BC_{pk} were closed because the mean of $\hat{\boldsymbol{\gamma}}_{G,j}$ for $j = 1, 2, \cdots, m$ were closed to the midpoint of the specification limits. For more information, interested readers are suggested to read Chiang et al. [3].

6 Conclusion

The main purpose of this chapter is to review the recent developments on the SPC to monitor SLP processes with correlated error terms; specially, SLP processes with within-profile autocorrelation. The common skill is to transform the SLP model with autocorrelated error terms to a SLP model with independent error terms and independent residuals so that the control charts for independent errors can be applied. Interested readers are suggested to read Chiang et al. [3] for potential research directions.

References

1. Borchers, H. W. (2018). *pracma: Practical numerical math functions*. R package version 2.1.8. https://CRAN.R-project.org/package=pracma
2. Castagliola, P., & Garcia Castellanos, J. V. (2005). Capability indices dedicated to the two quality characteristics case. *Quality Technology and Quantitative Management, 2*, 201–220.
3. Chiang, J.-Y., Lio, Y. L., & Tsai, T.-R. (2017). MEWMA control chart and process capability indices for simple linear profiles with within-profile autocorrelation. *Journal of Quality and Reliability Engineering International, 33*, 1083–1094.
4. Genz, A., Bretz, F., Miwa, T., Mi, X., Leisch, F., Scheipl, F., et al. (2018). *mvtnorm: Multivariate normal and t distributions*. R package version 1.0-8. http://CRAN.R-project.org/package=mvtnorm
5. Gupta, S., Montgomery, D., & Woodall, W. (2006). Performance evaluation of two methods for online monitoring of linear calibration profiles. *International Journal of Production Research, 44*, 1927–1942.
6. Jensen, W. A., Brich, J. B., & Wood, W. H. (2008). Monitoring correlation within linear profiles using mixed models. *Journal of Quality Technology, 40*, 167–183.
7. Kang, L., & Albin, S. (2000). On-line monitoring when the process yields a linear profile. *Journal of Quality Technology, 32*, 418–426.
8. Kim, K., Mahmoud, M. A., & Woodall, W. H. (2003). On the monitoring of linear profiles. *Journal of Quality Technology, 35*, 317–328.
9. Lowry, C. A., Woodall, W. H., Champ, C. W., & Rigdon, S. E. (1992). A multivariate exponentially weighted moving average control chart. *Technometrics, 34*, 46–53.
10. Mahmoud, M. A., Parker, P. A., Woodall, W. H., & Hawkins, D. M. (2007). A change point method for linear profile data. *Quality and Reliability Engineering International, 23*, 247–268.
11. Mestek, O., Pavlik, J., & Suchánek, M. (1994). Multivariate control charts: Control charts for calibration curves. *Fresenius' Journal of Analytical Chemistry, 350*, 344–351.
12. Noorossana, R., Amiri, A., & Soleimani, P. (2008). On the monitoring of autocorrelated linear profiles. *Communications in Statistics–Theory and Methods, 37*, 425–442.
13. Noorossana, R., Amiri, A., Vaghefi, S. A., & Roghanian, E. (2004). Monitoring quality characteristics using linear profile. In *Proceedings of the 3rd International Industrial Engineering Conference, Tehran, Iran*.
14. Saghaei, A., Mehrjoo, M., & Amiri, A. (2009). A CUSUM-based method for monitoring simple linear profiles. *The International Journal of Advanced Manufacturing Technology, 5*, 1252–1260.
15. Shahriari, H., Huebele, N. F., & Lawrence, F. P. (1995). A multivariate process capability vector. In *Proceeding of the 4th Industrial Engineering Research Conference* (pp. 304–309). Norcross: Institute of Industrial Engineers.
16. Soleimani, P., Noorossana, R., & Amiri, A. (2009). Simple linear profiles monitoring in the presence of within profile autocorrelation. *Computers & Industrial Engineering, 57*, 1015–1021.
17. Stover, F. S., & Brill, R. V. (1998). Statistical quality control applied to ion chromatography calibrations. *Journal of Chromatography A, 804*, 37–43.
18. Woodall, W. H., Spitzner, D. J., Montgomery, D. C., & Gupta, S. (2004). Using control charts to monitor process and product quality profiles. *Journal of Quality Technology, 36*, 309–320.
19. Zou, C., Zhang, Y., & Wang, Z. (2006). A control chart based on a change-point model for monitoring linear profiles. *IIE Transactions, 38*, 1093–1103.